



OPEN Kinematic signature of high risk labored breathing revealed by novel signal analysis

William B. Ashe^{1,5}, Brendan D. McNamara^{2,6}, Swet M. Patel^{2,6}, Julia N. Shanno^{3,7}, Sarah E. Innis^{3,7}, Camille J. Hochheimer⁴, Andrew J. Barros^{2,5}, Ronald D. Williams¹, Sarah J. Ratcliffe^{4,5}, J. Randall Moorman^{2,3,5} & Shrirang M. Gadrey^{2,5}✉

Breathing patterns (respiratory kinematics) contain vital prognostic information. This dimension of physiology is not captured by conventional vital signs. We sought to determine the feasibility and utility of quantifying respiratory kinematics. Using inertial sensors, we analyzed upper rib, lower rib, and abdominal motion of 108 patients with respiratory symptoms during a hospital encounter (582 two-minute recordings). We extracted 34 features based on an explainable correspondence with well-established breathing patterns. K-means clustering revealed that respiratory kinematics had three dimensions apart from the respiratory rate. We represented these dimensions using respiratory rate variability, respiratory alternans (rib-predominant breaths alternating with abdomen-predominant ones), and recruitment of accessory muscles (increased upper rib excursion). Latent profile analysis of the kinematic measures revealed two profiles consistent with the established clinical constructs of labored and unlabored breathing. In logistic regression, the labored breathing profile improved model discrimination for critical illness beyond the Sequential Organ Failure Assessment (SOFA) score (AUROC 0.77 vs 0.72; $p = 0.02$). These findings quantitatively confirm the prior understanding that the respiratory rate alone does not adequately represent the complexity of respiratory kinematics; they demonstrate that high-dimensional signatures of labored breathing can be quantified in routine practice settings, and they can improve predictions of clinical deterioration.

Keywords Respiratory Failure, Physiological Monitoring, Work of Breathing, Early Warning Scores, Biomedical Engineering

Breathing patterns (or respiratory kinematics) contain vital diagnostic and prognostic information. The normal breathing pattern is slow, regular cycles, usually 8–20 per minute, and a stable phenotype of predominantly abdominal or lower thoracic motion. These features make for an unmistakably effortless appearance. To clinicians, a normal breathing pattern is an important and reassuring physical examination finding¹. In contrast, abnormal breathing patterns are important markers of disease².

Labored breathing patterns, for example, are physical examination signs of an increased work of breathing³. They are considered to be red-flag signs which often herald clinical deterioration⁴. Labored breathing patterns include abnormalities of rate, rhythm, and relative movements of the upper chest, lower chest, and abdomen. Increased respiratory rate, or tachypnea, is an important feature of labored breathing. Its association with clinical deterioration is well known, as evidenced by its use in prominent criteria like quick Sequential Organ Failure Assessment (qSOFA) and National Early Warning Score (NEWS)^{5,6}. Additionally, the rhythm of labored breathing can be unusually irregular^{7,8}. More subtle but equally important are abnormalities in the relative movements of the chest and abdomen. It is abnormal for the major motion of breathing to alternate between the chest and the abdomen; it signifies an overload of the primary respiratory muscles (diaphragm and intercostal)⁹. It is also abnormal for the upper chest to have large excursions during breaths; it signifies increased recruitment of accessory respiratory muscles in the neck (sternocleidomastoid and scalene)⁹. Many such breathing patterns

¹Department of Electrical and Computer Engineering, University of Virginia, Charlottesville, USA. ²Department of Medicine, University of Virginia, Charlottesville, USA. ³Department of Biomedical Engineering, University of Virginia, Charlottesville, USA. ⁴Department of Public Health Sciences, University of Virginia, Charlottesville, USA. ⁵Center for Advanced Medical Analytics, University of Virginia, Charlottesville, USA. ⁶These authors contributed equally: Brendan D. McNamara and Swet M. Patel. ⁷These authors contributed equally: Julia N. Shanno and Sarah E. Innis. ✉email: smg7t@virginia.edu

have been linked to the work of breathing. However, a precise operational definition for the overarching construct of labored breathing has remained elusive.

Conventional vital signs do not report on respiratory kinematics beyond the average respiratory rate, and clinicians rely on qualitative visual inspections for a complete assessment of high risk breathing patterns¹⁰. Such assessments lack sensitivity and inter-rater reliability¹¹, and they are manual effort intensive. Methods like plethysmography (inductance or optoelectronic) allow automated, quantitative analysis^{9,12,13}. Their use has remained largely confined to specialized laboratories¹⁴. In routine clinical settings, respiratory kinematic information has not yet been quantified on a scale required for predictive modelling¹⁴.

We previously developed time-series methods to detect breath intervals and characterize respiratory kinematics using inertial sensors in healthy adults in an exercise physiology laboratory¹⁵. Here, we evaluated these respiratory kinematic characteristics at the hospital bedside. We describe a clinically explainable, high-dimensional signature of labored breathing, and validate it as a physiomaer of clinical deterioration during hospital encounters.

Methods

This study was approved by University of Virginia Health Sciences Institutional Review Board (study number 20844). All study procedures were performed in accordance with relevant guidelines and regulations, and informed consent was obtained from all subjects. We recruited 121 adults during a hospital encounter for dyspnea. We excluded patients with neuro-cognitive impairments and those requiring mechanical ventilation (non-invasive / invasive) that alters respiratory kinematics at the time of screening. We recorded demographics, comorbidities, and severity of illness in the span of 24 h from the kinematic recording (discharge home vs. non-critical care in hospital vs. critical care in hospital). We defined critical care as admission to an intensive care unit (ICU) or ICU level interventions (invasive or non-invasive mechanical ventilation, fraction of inspired oxygen > 50%, or cardiopulmonary resuscitation).

Kinematic recording apparatus and signal processing

To record respiratory kinematics, we used the MbitLab MetaMotion R inertial sensors which contain Bosch BMI160 inertial measurement units. We made recordings at 6 locations: midline sternal head, bilateral second rib in the midclavicular line, bilateral eighth rib in the anterior axillary line, and midline abdomen. At each location, we analyzed three axes each of accelerometer and gyroscope signals (sampling frequency: 100 Hz). Multiple two-minute recordings were obtained over 6 h (number of recordings and the intervals between them varied by clinical circumstances; details in supplement Sect. 1). We used non-causal band-pass filtering (corner frequencies: 0.05 and 1 Hz). We used 4th and 6th order Butterworth kernels for the low and high filters, respectively; we achieved zero-phase filtering with forward-backward filtering, resulting in a filter strength of 8th and 12th orders.

Feature extraction: Respiratory rate series

After filtering, we separated breaths using the phase angle from the analytic representation of the signals. The analytic representation is a complex plane where the Hilbert transform of a signal is represented on the imaginary y-axis as a function of the untransformed signal on the real x-axis. The phase of any point of the analytic signal is the angle between a line joining that point to the origin and the positive x-axis. We used phase landmarks to identify breath intervals and to extract an interpolated instantaneous respiratory rate series from each of the 36 signal streams (6 streams per sensor x 6 sensors)^{15,16}. In noise-free segments, the rate series converged on the true respiratory rate. In noisy segments, there was no convergence. We considered the signal clean if a majority (≥ 18) of the rates clustered together. We deemed a recording as acceptable if ≥ 30 s of the recording was clean. This process is depicted in Fig. 1 (and in the supplement Sect. 2). In clean segments, we used the centroid of convergent rates as the final respiratory rate. To assess the rate of breathing, we measured the mean of the kinematics-derived respiratory rate series. To assess the rhythm of breathing, we measured the dispersion of the kinematics-derived respiratory rate series (standard deviation and coefficient of variation of the respiratory rate time series, and 9 other measures; details in supplement Sect. 4).

External validation of the respiratory rate series

To validate our respiratory rate series, we applied it to 60 respiratory kinematic signals that were recorded in synchrony with volumetric air flow signals during our previous study in an exercise physiology lab (EPL)¹⁵. We compared the kinematics-derived and flow-derived mean respiratory rates using the Bland-Altman method. We calculated the cross-correlation coefficients between kinematics-derived and flow-derived respiratory rate time series (details in supplement Sect. 3).

Feature extraction: Signal amplitude series

We extracted instantaneous amplitude time series from the linear acceleration signals to measure features of the relative movements of the chest and the abdomen (Fig. 2; supplement Sect. 3). The instantaneous amplitude of any point in a signal is the magnitude (distance from origin) of the corresponding point in the analytic representation of that signal (Fig. 1E). This method allowed us to assess: (a) the average magnitude of movement at a certain location of the torso (e.g., to what extent do the upper ribs move during breathing), (b) the average relationship between movements at two locations (e.g., on average, is breathing rib dominant or abdomen dominant or mixed), and the (c) the degree of variability in the relationship between movements at two locations (e.g., do rib dominant breaths alternate with abdomen dominant breaths).

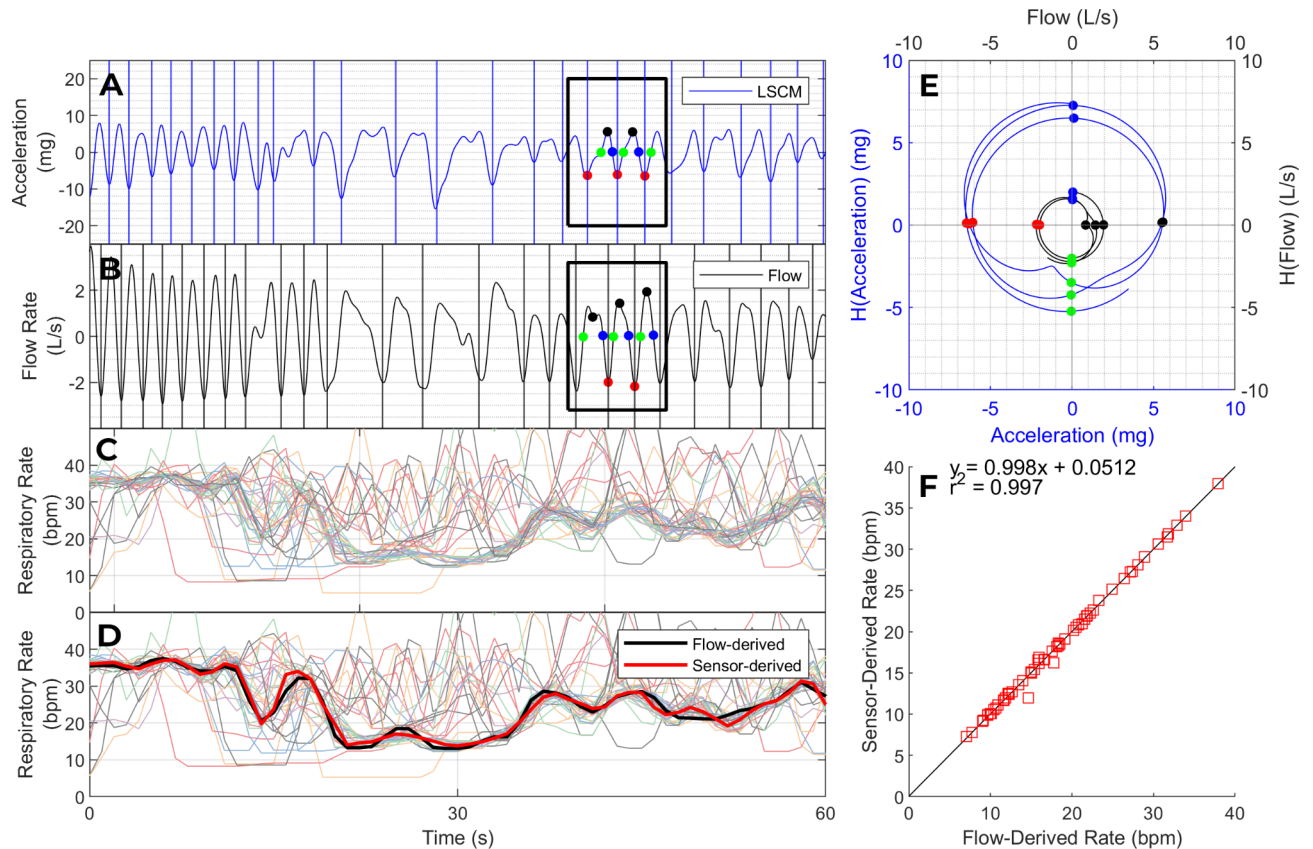
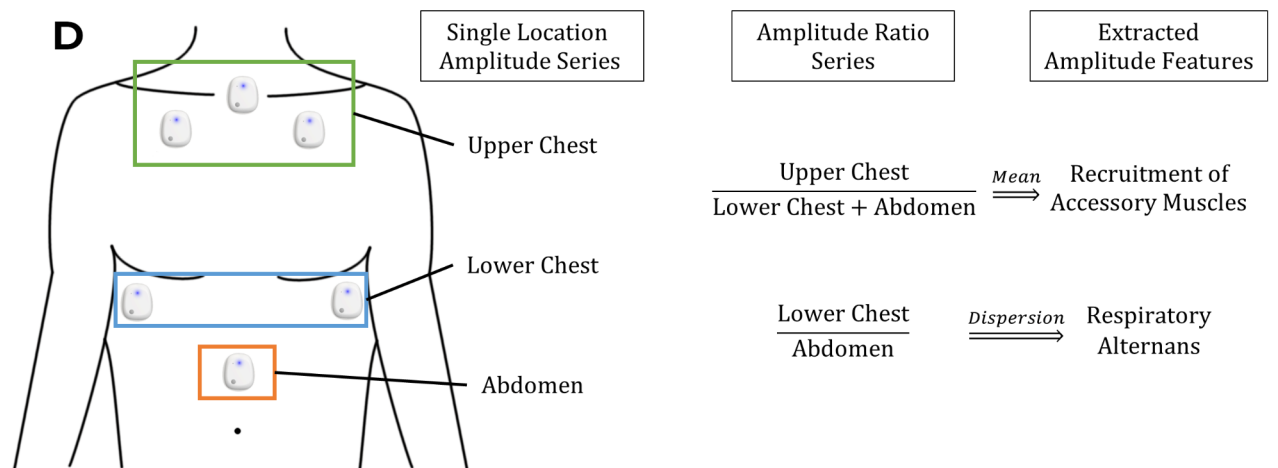
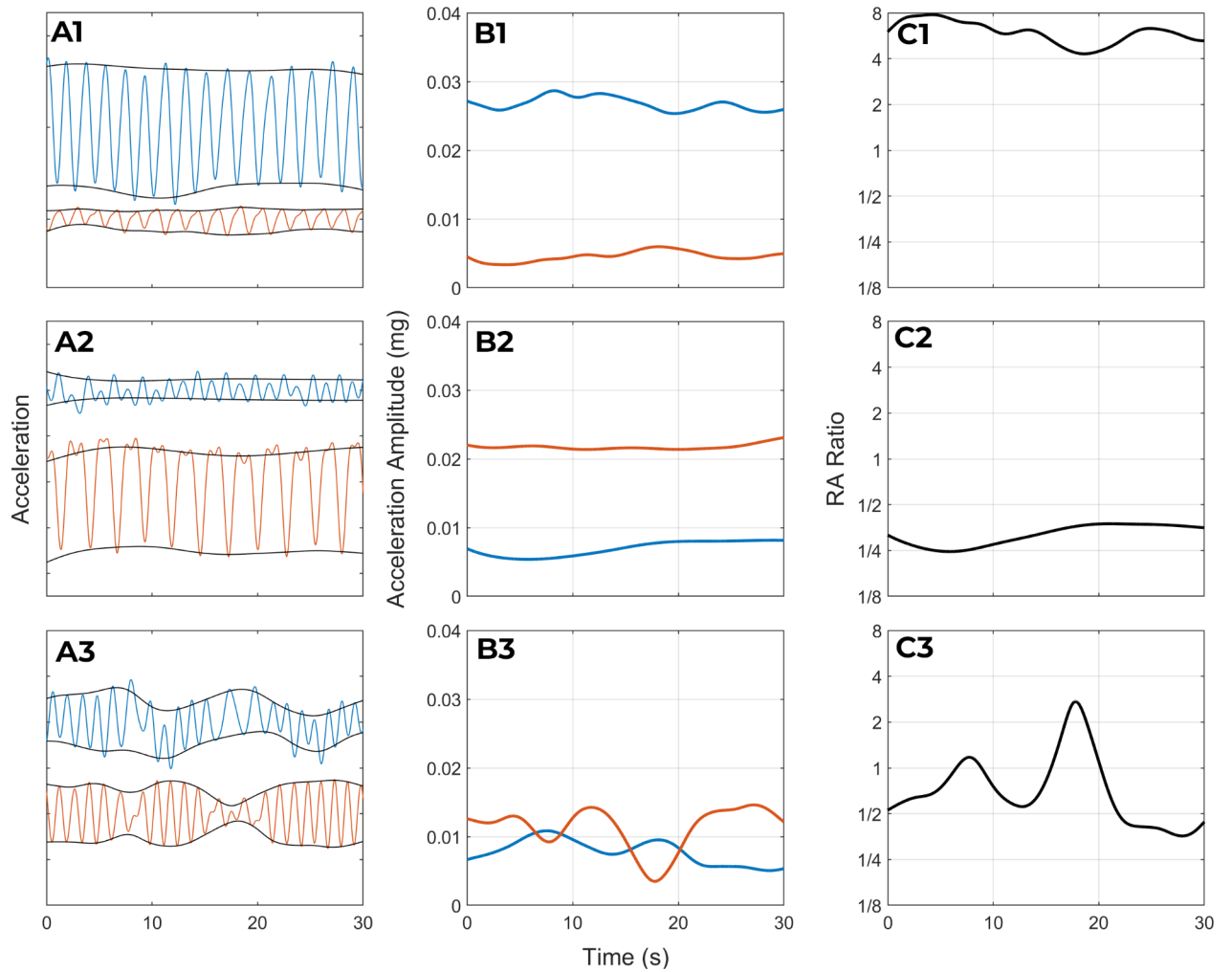


Fig. 1. Respiratory rate and rhythm. Panels A and B show a respiratory kinematic signal from an accelerometer (A) and a synchronized volumetric air flow signal (B). The colored dots correspond to phase landmarks in the analytic representation of these signals (E), evenly spaced in phase at intervals of $\pi/2$ radians. The phase of any point of the analytic signal (E) is the angle between a line joining that point to the origin and the positive x-axis. We used analytic phase landmarks to identify breath intervals and to extract an interpolated instantaneous respiratory rate series from each kinematic signal. Panel C shows 36 interpolated respiratory rate time series from one patient (6 kinematic signals per location; 6 locations). The rates extracted from clean kinematic signals converged on the true respiratory rate whereas the rates extracted from noisy kinematic signals deviated from the true respiratory rate to a varying degree. We identified the largest cluster of converging respiratory rates (thick bundle in Panel C) and adjudicated its centroid as our estimate of the respiratory rate (black line in Panel D). The final kinematics-derived rate series (black line) matched the flow-derived rate series (red line) with high fidelity. Panel F plots the kinematics-derived respiratory rate as a function of flow-derived respiratory rate in 60 paired recordings, with 95% limits of agreement of ± 0.9 breaths per minute.

Feature selection and latent profile analysis

In all, we extracted the average respiratory rate and 33 novel metrics from each recording: 11 metrics that reported on the rhythm of breathing, and 22 metrics that reported on the relative movements of the sensor locations (details in supplement Sect. 4). We selected mean respiratory rate based on its clinical import. We applied k-means clustering to the remaining 33 metrics to determine how many and which of the features should be selected to represent the observed respiratory kinematic variability in our dataset. We determined the number of features to use by looking for an “elbow” in the Within Sum of Squares (WSS) plot. We decided to select metrics from different clusters to avoid selecting multiple features that captured overlapping information (e.g., features that turn out to be highly correlated). We selected the metrics with the most well-established link to work of breathing in the bedside diagnosis and physiological laboratory literature. This process is detailed further in supplement Sect. 5. We avoided a purely clinically-driven feature selection approach to minimize arbitrary choices as much as possible. We avoided a supervised data-driven feature selection approach to avoid the problem of spurious associations due to multiple comparisons.

To uncover high-dimensional breathing pattern phenotypes, we applied latent profile analysis (LPA) to the selected measures (supplement Sect. 5). We determined the number of profiles to create based on a plateau (“elbow”) in Bayesian Information Criterion (BIC) improvement. We identified the profile consistent with the clinical construct of labored breathing. Each recording was thereby classified as either labored or unlabored breathing. For each patient, we calculated the proportion of their recordings that were classified as labored breathing (i.e., the frequency of labored breathing).



Statistical analysis

We used Poisson regression to assess the relationship between the frequency of labored breathing and the severity of their illness. This approach accounted for variability in number of recordings per patient. Further, we used logistic regression to assess whether the frequency of labored breathing, plus each feature independently, improved model discrimination (area under receiver operator characteristic curve or AUROC) for critical illness beyond the Sequential Organ Failure Assessment (SOFA) score^{5,17}.

The SOFA score is calculated every 15 min at the University of Virginia Medical Center using methods that have been previously described¹⁸. The renal, hepatic, and coagulation components are updated every time a new result of a pertinent laboratory test is available (creatinine, total bilirubin, and platelet count respectively). The cardiovascular and neurologic components are updated every time a new entry of a pertinent vital sign (blood pressure), medication administration record (vasopressors) or nursing assessment (Glasgow Coma Scale)

◀ **Fig. 2.** Relative movements of the chest and abdomen. This figure illustrates the information contained in the amplitude-relationships between the kinematic signals by displaying the signals of three patients (rows 1–3) whose breathing pattern varied in this regard. The first column of panels (A1–A3) shows one accelerometer signal from the lower rib (blue) and abdominal (orange) sensor of each patient. The instantaneous amplitude series of the signals in A1–A3 is plotted in panels B1–B3 respectively. Panels C1–C3 show the amplitude ratio series that is obtained by dividing the lower rib amplitude series by the abdominal amplitude series in B1–B3. The first patient (Row 1) has a stable phenotype of rib-predominant breathing: the lower rib sensor (blue) has a higher amplitude kinematic signal than the abdominal sensor (orange) in A1; the lower rib (blue) has higher instantaneous amplitude than the abdomen (orange) in B1; and the amplitude ratio series in C1 has a mean value greater than 1. In contrast to the rib-predominant breathing of the first patient, the second patient (Row 2) has abdomen-predominant breathing (A2 and B2) which results in an amplitude ratio that is less than 1 (C2). Despite their different breathing patterns, both of these patients have a stable pattern from one breath to the next. As a result, their amplitude ratio time series (C1 and C2) have low variability. In contrast, the third patient (row 3) has an unstable breathing pattern where rib predominant breaths alternate with abdomen predominant ones. This results in an amplitude ratio time series (C3) with high variability. Panel D schematically represents the derivation of our measures for respiratory alternans and recruitment of accessory muscle.

is available. The respiratory component is calculated using a previously validated method to non-invasively estimate the P/F ratio^{19,20}. It is updated every time a new pulse oximetry result or oxygen supplementation setting is available. If no new data are available for a given component, the last known value is carried forward for up to 12 h. In this study, we used the patient's highest recorded SOFA score in the 12 h before the final respiratory kinematic recording.

Results

Signal quality and cohort characteristics

We successfully recorded 790 high-quality two-minute inertial signals from 108 of the 121 patients during their hospital encounter for shortness of breath. 582 (74%) of the 790 recordings met our acceptability criterion; at least 30 s of these 582 recordings was free of non-respiratory motion artefacts. In the remaining 208 recordings, notwithstanding the high-quality inertial signal, fewer than 30 s was free of non-respiratory motion capture. Each of the 108 patients had at least 1 acceptable recording, and the median number of acceptable recordings per patient was 5 (range 1–11). In all, 717 min of noise-free inertial signal was used in the final analysis from 582 recordings (an average of 1.23 min per two-minute recording).

The demographic, clinical, and outcome data from our cohort are detailed in Table 1. At least one chronic pulmonary condition was present in 42% of the patients ($n=46$). Chronic obstructive pulmonary disease ($n=35$) and asthma ($n=15$) were the most common chronic conditions. Other diagnoses ($n=13$) included interstitial lung disease, bronchiectasis, lung cancer, and sarcoidosis; some patients had more than one diagnosis. Of the 582 recordings, 120 (21%) were from the 26 patients that required critical-care hospitalization, 355 (61%) were from the 60 patients that required acute-care hospitalizations, and 107 (18%) were from the 22 patients that were discharged home.

Examples of signal analysis

Figure 1 illustrates our method of assessing the rate and rhythm of breathing. This method performed well in our external validation dataset (supplement Sect. 3). Compared to the gold standard respiratory rate series (obtained using volumetric air flow sensors), the kinematics-derived respiratory rate series was highly accurate (bias: -0.02 breaths per minute; 95% limits of agreement: ± 0.9 breaths per minute; average cross correlation coefficient:

Age, median (range)	65 (19–91)
Sex (percentage)	
Female	54
Male	46
Race (percentage)	
White	85
Black	13
Other	2
SOFA score, median (range)	3.5 (0 to 11)
Severity of illness (percentage)	
Critical-care hospitalization	24
Acute-care hospitalization	56
Discharge home	20

Table 1. Patient characteristics.

0.89). Figure 2 illustrates our method of assessing the relative movements of the upper chest, lower chest, and abdomen by analyzing the instantaneous amplitudes of linear acceleration.

A latent profile of labored breathing

By applying k-means clustering^{21,22} to the 33 novel measures, we found that the elbow in the Within Sum of Squares (WSS) plot occurred with 3 clusters (Figure S6 in supplement Sect. 5). Based on this, we elected to represent the respiratory kinematic variability across the 582 recordings using 3 metrics, one each from a different K-means cluster (details in supplement Sect. 5). These measures correspond with respiratory rate variability (short breaths alternating with long ones), respiratory alternans (rib-predominant breaths alternating with abdomen-predominant or mixed breaths), and recruitment of accessory muscles (increased upper chest expansion caused by contraction of neck muscles like scalene and sternocleidomastoid). The metrics were not correlated with each other; correlation coefficients were under 0.2 in all pairs.

In the latent profile analysis^{23–25}, we determined that the data were most consistent with two latent phenotypes of breathing (details in supplement Sect. 5). One phenotype, had high means in all four metrics (respiratory rate: 24 bpm [70th percentile]; respiratory rate variability: 6.8 bpm [76th percentile]; respiratory alternans: 0.53 [74th percentile]; recruitment of accessory muscles: 1.9 [81st percentile]). This is consistent with the clinical construct of labored breathing. The other phenotype had lower mean values, consistent with unlabored breathing (respiratory rate: 20 bpm [42nd percentile]; respiratory rate variability: 4.6 bpm [46th percentile]; respiratory alternans: 0.37 [45th percentile]; recruitment of accessory muscles: 1.1 [42nd percentile]).

Statistical analysis

The overall frequency of the labored breathing phenotype was 33% (193 of 582 total recordings). Poisson regression revealed an association between the proportion of a patient's recordings that contained the labored breathing phenotype, and the severity of the patient's illness. The frequency of the labored breathing phenotype was lowest (21%) in patients who were discharged home. Compared to this group, the frequency of labored breathing was higher in patients who required non-critical care hospitalization (33% v/s 21%; $p=0.06$) and in patients requiring critical care hospitalization (44% v/s 21%; $p=0.004$).

Logistic regression revealed that the frequency of labored breathing was independently associated with critical illness even after adjusting for the SOFA score. Every percentage point increase in a patient's frequency of labored breathing was associated with an adjusted odds ratio of 1.02 ($p=0.02$). The frequency of labored breathing ranged from 0 to 100% in the 108 patients (mean 35%; standard deviation 32). Comparing patients with entirely labored and entirely unlabored breathing profiles (i.e., frequency of labored breathing of 100% and 0% respectively) that odds ratio for critical illness was 5.5 even after adjusting for the SOFA score. Model discrimination for critical illness (AUROC) improved significantly (0.72 to 0.77, $p=0.02$) when the frequency of labored breathing was added to the SOFA score in the logistic regression model. Mean recruitment of accessory muscles was the individual metric that improved model performance the most, but the performance improvement of individual metrics was not statistically significant (details in the supplement Sect. 6).

Further, as shown in Fig. 3, labored breathing was identified in 20% (48/242) non-tachypneic recordings. The re-classification of critical illness improved when the labored breathing phenotype was added to tachypnea as a marker of respiratory distress.

Clinical vignettes

Figures 4, 5 and 6 contain six respiratory kinematic recordings along with a narration of their clinical context. These cases were selected to illustrate the various scenarios where quantitative characterization of respiratory kinematics may significantly enhance medical decision making. For ease of illustration, we displayed a single kinematic stream at each sensor location that conveys the features that are measured by the metrics.

Figure 4 contains the respiratory kinematic recordings of two patients who presented with shortness of breath. Neither patient was tachypneic; both had a normal and virtually identical respiratory rate. However, only one of these patients exhibited a labored breathing phenotype. The patient with non-tachypneic and non-labored breathing was uneventfully discharged home. The patient with the non-tachypneic but labored breathing was admitted to the intensive care unit for life-threatening respiratory failure. This vignette demonstrates how high-risk labored breathing is detectable even in the absence of tachypnea.

Figure 5 also contains the respiratory kinematic recordings of two patients who were initially admitted to the acute care for the treatment of pneumonia and mild hypoxemic respiratory failure. Both patients were tachypneic, and the risk predicted by the Pneumonia Severity Index was comparable²⁶. However, the breathing patterns of one patient were more labored than the other (larger elevations in respiratory rate variability, recruitment of accessory muscles, and respiratory alternans). The patient with lower degrees of labored breathing derangements remained stable and was uneventfully discharged home after recovery. The patient with higher degrees of labored breathing derangements developed an abrupt clinical deterioration requiring an emergent endotracheal intubation and an unplanned transfer to the intensive care unit for life-threatening respiratory failure. That patient died within 24 h of their respiratory kinematic recording. This vignette exemplifies the clinical scenario where respiratory kinematic characteristics may provide alerts that are more specific than tachypnea for respiratory muscle overload and imminent respiratory deterioration.

Figure 6 contains two respiratory kinematic recordings obtained from one asthmatic patient whose acute respiratory failure resolved rapidly after breathing treatments were administered. The recordings show improvements in the patient's respiratory kinematic characteristics that match their clinical trajectory. This vignette highlights how respiratory kinematic characteristics can reveal dynamic pathophysiological trends²⁷.

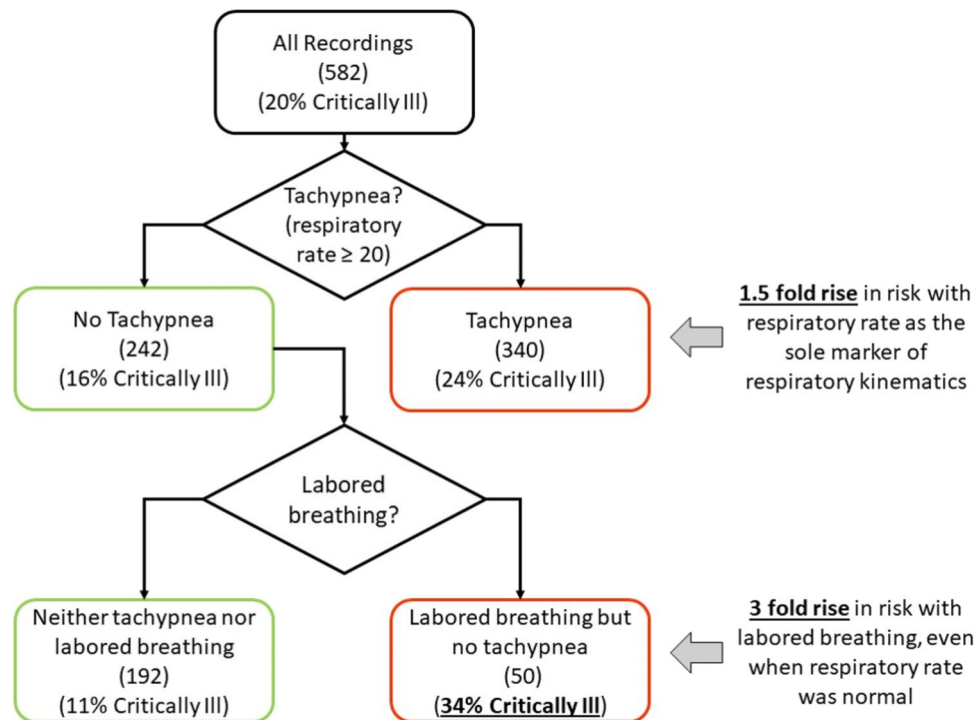


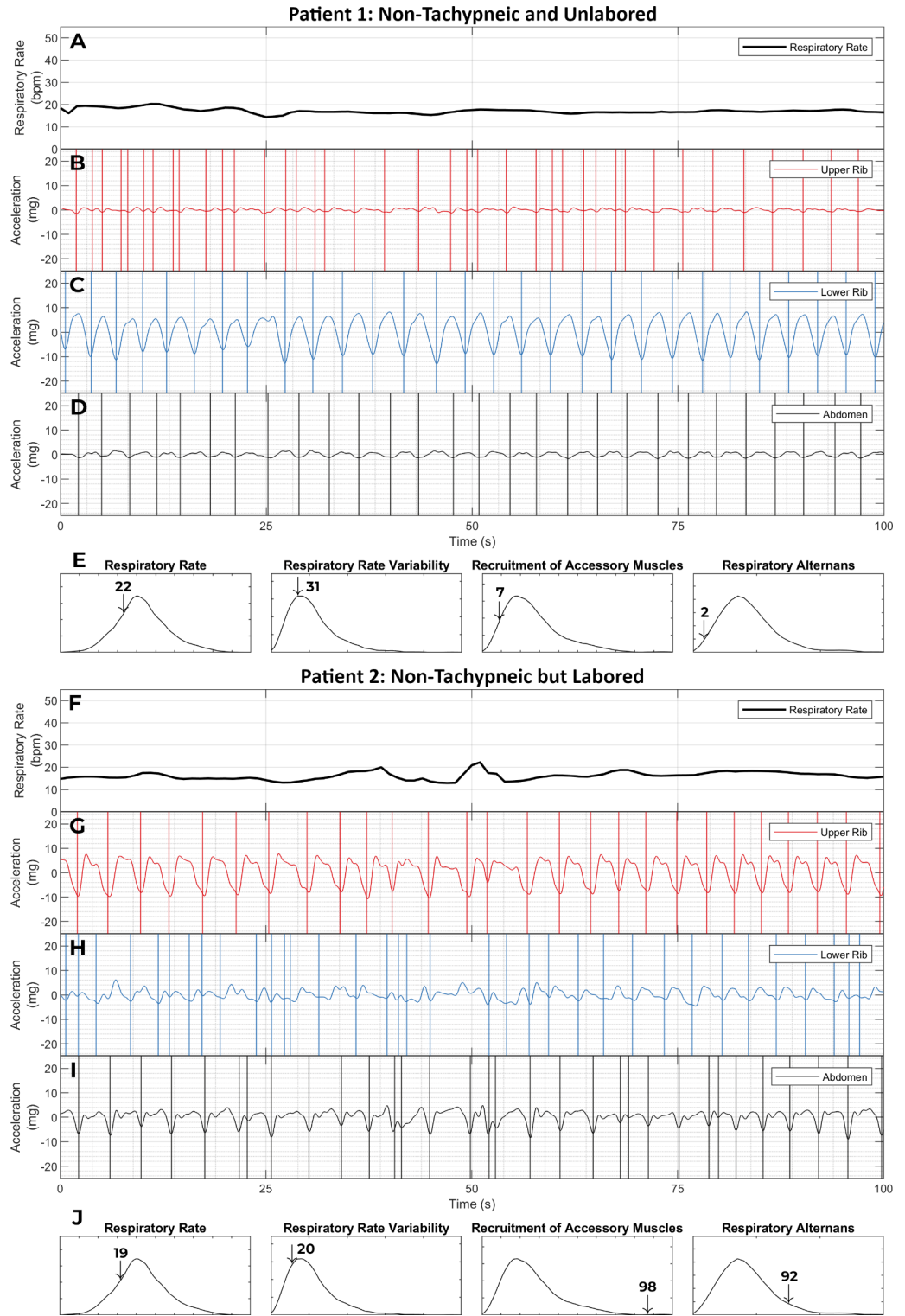
Fig. 3. Labored breathing phenotype improved model discrimination for critical illness. Multi-dimensional analysis of respiratory kinematics revealed a signature of labored breathing that was associated the severity of illness. The statistical significance of this association was demonstrated by Poisson and logistic regression. The clinical significance of that association is conveyed by this figure. Of the 582 recordings, 20% belonged to patients who required critical care hospitalization. When we used respiratory rate as the sole respiratory kinematic physiometer (which is the prevailing clinical standard), tachypnea (respiratory rate ≥ 20 breaths per minute) was associated with a 1.5-fold rise in risk of critical illness (24% v/s 16%). Arguably, this is classification alone is clinically useful and affirms the validity of the kinematics-derived respiratory rate. Importantly, however, the classification improved when the low-risk (non-tachypneic) recordings were further separated based on the presence of the labored breathing. More than one fifth of the 242 non-tachypneic recordings contained the labored breathing phenotype. These recordings were associated with a 3-fold rise in risk of critical illness when compared to the non-tachypneic non-labored recordings (34% v/s 11%).

Discussion

We studied the breathing motion patterns of patients with active respiratory symptoms. Our major findings are that (a) respiratory kinematics are a rich source of quantifiable physiological information, with more complexity than is adequately represented by the respiratory rate alone, and (b) high-risk respiratory kinematic phenotypes can be quantified in routine practice settings through multi-dimensional analysis of respiratory kinematics.

Clinicians have long recognized that the respiratory rate is an important vital sign. Equally well understood is the degree of inaccuracy with which it is currently measured^{28,29}. We derived a method for respiratory rate estimation in our hospital patient population and validated that it results in highly accurate estimates in new populations (bias and 95% limit of agreement of -0.02 ± 0.9 breaths per minute in the exercise physiology laboratory subjects). Improving the accuracy of respiratory rate documentation can enhance patient safety, especially in the more remote parts of the world. For example, approximately 750,000 children under 5 years of age die from pneumonia every year³⁰. UNICEF estimates that many deaths can be prevented if parents and community health workers can simply be trained to measure the respiratory rate and detect tachypnea³¹. But even this basic assessment (fast vs. normal respiratory rate) cannot be reliably achieved in many parts of the world³². The respiratory rate estimation methods described in this paper may improve diagnosis and save lives.

Notwithstanding the importance of the respiratory rate, it is only one among many breathing motion patterns that convey respiratory distress. A patient's breathing can exhibit high-risk labored breathing despite a normal respiratory rate. In such scenarios, the risk can be captured by detecting other abnormal patterns like excessive upper rib excursion during breathing or an unstable breath phenotype (chest predominant breaths alternating with abdomen predominant ones). Seasoned clinicians caution their trainees, therefore, against the use of respiratory rate as the sole marker of labored breathing³. In the absence of quantitative clinical and research tools, however, such insights have been largely restricted to the domain of conventional clinical wisdom. A major contribution of our study is to quantitatively confirm this prevailing clinical intuition and provide one of the first estimates of its magnitude in a real-world clinical setting. Our novel physiometers revealed signs of labored breathing in a fifth of the recordings that had a normal respiratory rate, even when we used one of the most sensitive clinical definitions of tachypnea (respiratory rate ≥ 20 breaths per minute). The resulting



reclassification led to improved model discrimination for critical illness. This points to a major opportunity for improvement in clinical risk stratification and early warning scores. Unanticipated respiratory compromise and unplanned intubation are common and catastrophic events in patients hospitalized in general medical and surgical units of a hospital^{33,34}. Early warnings triggered by high-risk respiratory kinematic phenotypes may empower clinicians to address this menacing problem.

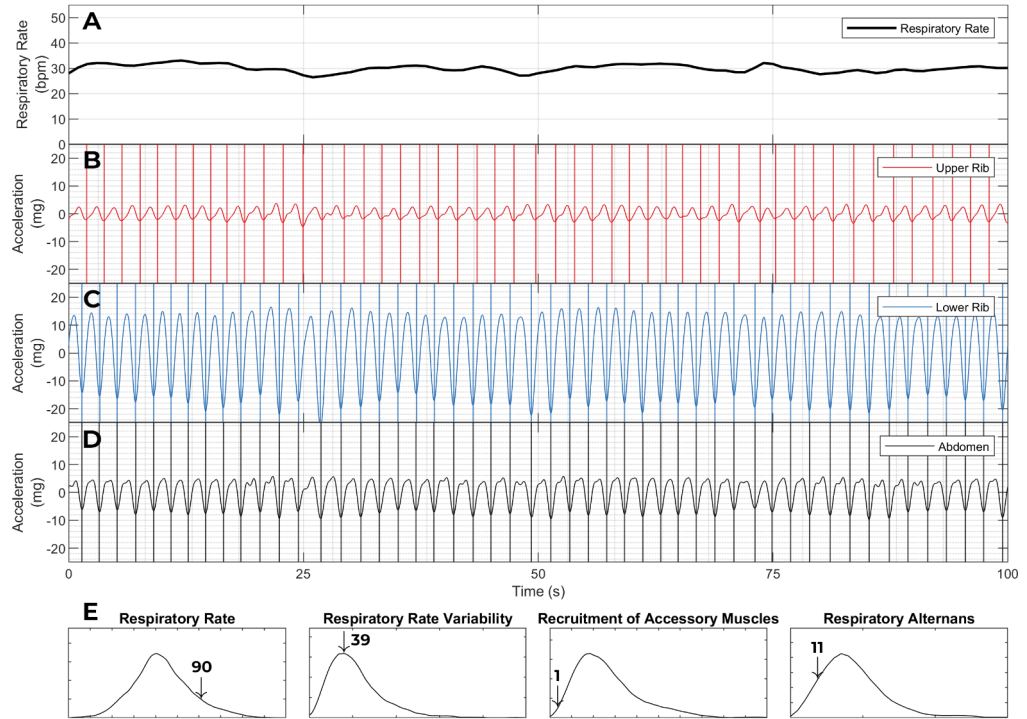
A major strength of this work is that it builds on principles that are fundamental to bedside diagnosis and to the pathophysiology of human ventilation. The physiomechanical extraction was clinically-driven. As such, the respiratory kinematic characteristics reported in this study have an easily explainable correspondence with physical examination signs that are commonly used by clinicians. Additional clinically-driven kinematic signal analysis can lead to a more comprehensive characterization of respiratory kinematics. Thoraco-abdominal asynchrony (“abdominal paradox”), Cheyne-Stokes breathing, and apneas are examples of well-known

◀ **Fig. 4.** Labored breathing without tachypnea. This figure shows the respiratory kinematic recordings of two patients with a normal respiratory rate (≤ 20 breaths per minute). Patient 1 (panels A - E) was a 77-year-old female who presented to the emergency room with shortness of breath. She exhibited not only a normal respiratory rate (22nd percentile in our dataset) but also an entirely unlabored breathing phenotype. Her breath intervals were regular. This was captured by a low respiratory rate variability (31st percentile). Her upper rib motion amplitude was low. This led to a low value on the recruitment of accessory muscles metric (7th percentile). And finally, she had a stable phenotype of lower rib dominant breathing. As a result, her respiratory alternans metric was also low (2nd percentile). Her emergency room workup was negative for any major acute illness. She was diagnosed with a viral upper respiratory infection and discharged home from the emergency room. Patient 2 (panels F - J) was a 57-year-old male who presented with shortness of breath and lethargy. Patient 2 also had a normal respiratory rate (19th percentile) and a low respiratory rate variability (20th percentile). Yet, he was classified as having labored breathing. This was driven by the recruitment of accessory muscle and respiratory alternans metrics which were at the 99th and 92nd percentiles. The elevated respiratory alternans metric resulted from the variable abdominal signal amplitude relative to a constant lower rib amplitude. The elevated recruitment of accessory muscles metric corresponds with the fact that the amplitude of the upper rib signal exceeds that of the lower rib or abdominal signals. He was found to have acute on chronic hypoxemic and hypercarbic respiratory failure from severe chronic obstructive pulmonary disease. He required 15 L per minute supplemental oxygen to maintain $\text{SpO}_2 > 88\%$; his pH was 7.2 and pCO_2 was 105. He was initiated on corticosteroids, antibiotics, non-invasive positive pressure ventilation and admitted to the ICU (not intubated only due to his advanced directive). These examples show how a high-dimensional analysis of respiratory kinematics can improve discrimination for critical illness. [SpO_2 : oxygen saturation on pulse oximetry; pH: potential of hydrogen; pCO_2 : partial pressure of carbon dioxide; ICU: intensive care unit]

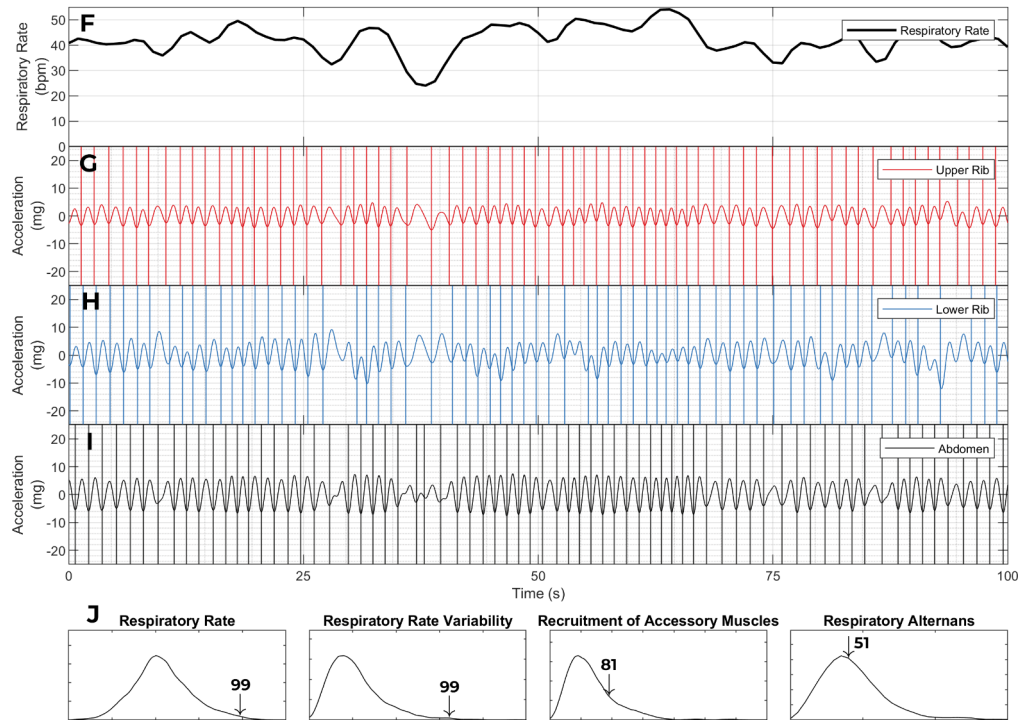
physical examination findings that were not operationalized in this study. Moreover, a data-driven approach to physiomechanics extraction may also be useful when larger respiratory kinematic datasets become available. In this latter approach, physiomechanics selection would be based on either an association with clinical outcomes (supervised learning), or an observed pattern in unlabeled data (unsupervised learning). Such physiomechanics may be poorly understood at first, but they may generate hypotheses and lead to the discovery of new pathophysiological mechanisms. Another strength of our work is that acceptable recordings were unobtrusively achieved in a busy hospital environment. Every patient had at least 1 acceptable recording and 75% of all recordings were acceptable. This demonstrates the technical feasibility of large scale respiratory kinematic monitoring in real-world clinical settings.

This study is limited in generalizability because of convenience sampling. Also, due to the small sample size, we encountered the problem of an unfavorable EPV (events per variable). We preselected two candidate predictors based on clinical domain knowledge, favoring summary predictors to save degrees of freedom^{35,36}. It is a limitation, nonetheless, that the study was not able to adjust for any pertinent variable other than respiratory kinematics and the Sequential Organ Failure Assessment (SOFA) score (such as age, sex, race, comorbidities, and non-respiratory vital signs like heart rate or temperature). Further, the present study does not address the variations in signatures of labored breathing related to the etiology of dyspnea or to willful manipulation by the subject (e.g., malingering). Finally, the study does not address factors of respiratory kinematic analysis that pertain to hardware or implementation science (e.g., form factor of sensors, ease of use, or practicality of sensors across the torso). Here, we demonstrate the technical feasibility and clinical utility of a novel signal analysis approach to respiratory physiological monitoring.

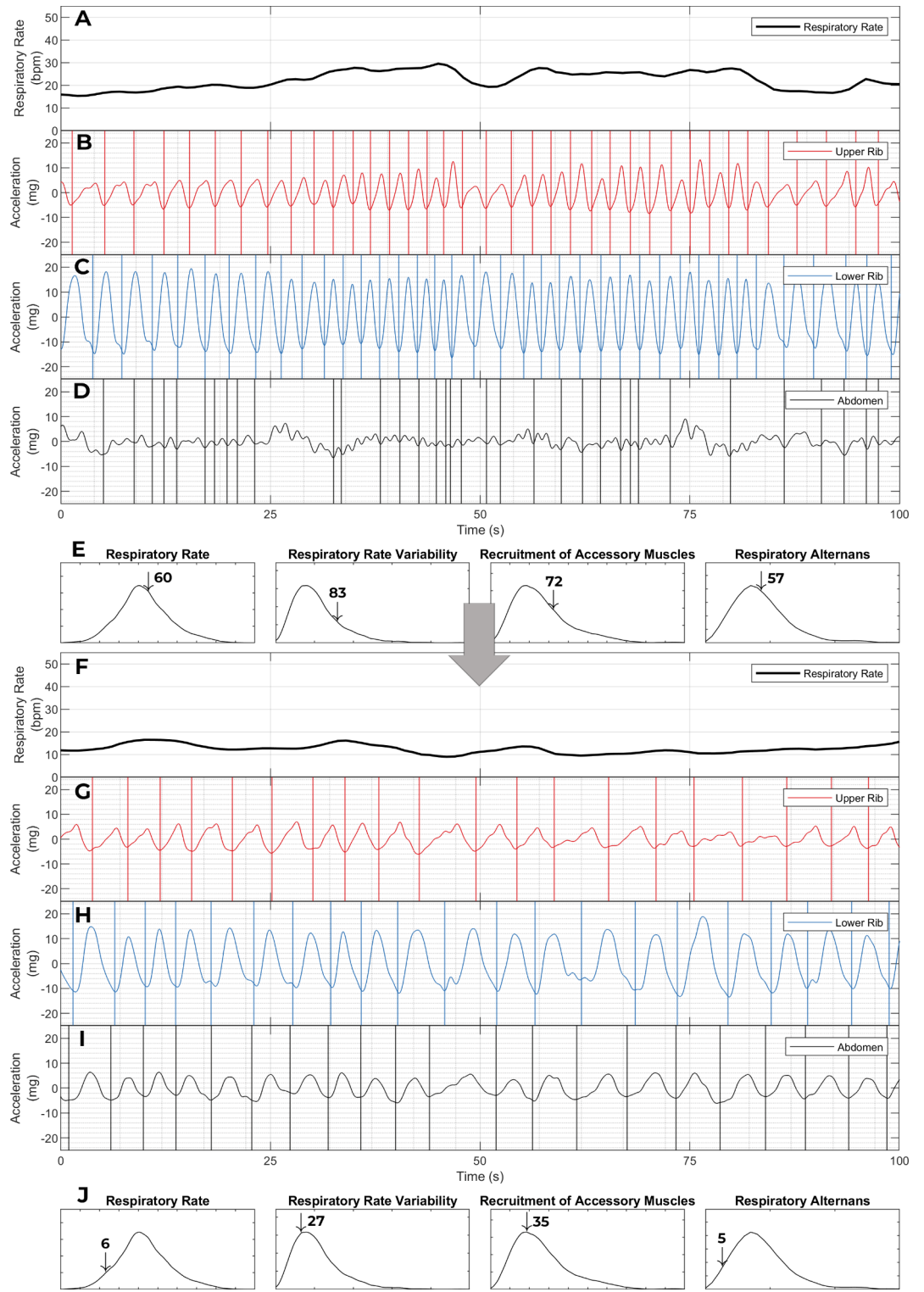
Patient 1: Lower-grade Derangements in Non-Tachypnea Physiometers



Patient 2: Higher-grade Derangements in All Labored-Breathing Physiometers



◀ **Fig. 5.** Respiratory muscle overload and imminent respiratory collapse. This figure shows the respiratory kinematic recordings of two female patients with elevated respiratory rates (90th and 99th percentiles for our dataset). They were both initially admitted to the acute care unit of the hospital for pneumonia and sepsis with acute respiratory failure. At admission, their supplemental oxygen needs were low (4 and 2 L per minute) and their blood gas studies were normal (pH of 7.43 and 7.44; pCO₂ of 33 and 40 mmHg). Their Pneumonia Severity Index scores were also comparable at 127 and 125 [scores of 91–130 are Risk Class 4 (moderate risk) and are associated with a 30-day mortality of 9%]. Apart from tachypnea and hypoxemia, the drivers of risk were age, hyponatremia, and confusion in patient 1, and fevers, anemia, and neoplastic disease (acute myelogenous leukemia) in patient 2. Despite the similarities in these patients' presentations and conventional risk levels, their clinically trajectories were dramatically different. Patient 1 remained stable on the acute care unit after her kinematic recording and was discharged home after a 7-day hospitalization. In contrast, Patient 2 developed a sudden respiratory collapse within 6 h of her kinematic recording (required emergent intubation), and died within 24 h of this recording. Severe hypoventilation from respiratory muscle overload was deemed to be the likely mechanism of the collapse; this conclusion was consistent with the rapidity of collapse, unresponsiveness to oxygen supplementation prior to intubation (low SpO₂ despite 100% FiO₂), and acute hypercapnia (pH 6.9 mm Hg; pCO₂ 103 mm Hg). A majority of both patients' recordings were classified as labored breathing in the latent profile analysis (3 of 4 recordings in patient 1, and 3 of 3 recordings in patient 2). However, a comparison of the respiratory kinematic characteristics of these patients revealed an important difference. Patient 1 (the survivor) had lower grade derangements in all non-tachypnea physiometers than the deceased patient 2. The breath intervals were more regular in Panels B-D than in panels G-I (respiratory rate variability at 39th percentile in panel E vs. 99th percentile in panel J). The upper rib motion amplitude was much smaller than lower rib or abdominal motion amplitude in panels B-D than in panels G-I (recruitment of accessory muscles at 1st percentile in panel G vs. 81st percentile in panel J). And the breath phenotype was much more stable in patient 1 than in patient 2. Each breath had a same degree of lower rib dominance in panels C-D, whereas rib dominant breaths alternated with abdomen dominant ones in panels H-I (respiratory alternans at 11th percentile in panel E vs. 51st percentile in panel J). Consistent with the conventional wisdom in the field of bedside physical diagnosis, these findings suggest that respiratory kinematic characteristics contain signatures that are much more specific for respiratory muscle overload than just tachypnea.



◀ **Fig. 6.** Personalized respiratory kinematic profiles and their trajectories. This figure contains two respiratory kinematic recordings of a 20-year-old male who presented with common cold symptoms and shortness of breath. He was diagnosed with acute hypoxemic respiratory failure (required up to 10 L per minute of supplemental oxygen) from an acute exacerbation of his mild intermittent asthma precipitated by a rhinovirus infection. With steroids and bronchodilator treatments, his hypoxemic respiratory failure rapidly resolved; his oxygen supplementation was stopped within 12 h of treatment and he was discharged after a 48-hour acute care hospitalization. Only one (the first) of his four recordings was classified as labored breathing in our unsupervised latent profile analysis. Trends consistent with the clinical trajectory can be seen in the two recordings shown here. In the initial recording (top) patient's breath intervals are shorter and more irregular than in the later recording (bottom). This corresponds with an improvement in our measures for respiratory rate (22 breaths per minute [60th percentile] to 12 breaths per minute [6th percentile]), and respiratory rate variability [83rd percentile to 27th percentile]. Note also, how the amplitude of upper rib signal improves (recruitment of accessory muscles metric goes from 72nd percentile to 35th percentile). Interestingly, this corresponds with an increase in the amplitude of the abdominal signal (In Panel D, there is virtually no organized abdominal signal; In Panel I, the abdominal signal is organized and its amplitude is higher than the upper rib). During an asthma exacerbation, dynamic hyperinflation can flatten the diaphragm and impair its contraction²⁷. Reduction in hyperinflation in response to treatment is a plausible explanation for such a change in kinematic recordings. This case highlights the potential for personalized respiratory kinematic profiling, whereby dynamic trends that deviate from an individual's own baseline profile may provide early warnings of acute illness.

Data availability

The datasets used and/or analyzed during the current study available from the corresponding author on reasonable request.

Received: 14 March 2024; Accepted: 25 October 2024

Published online: 13 November 2024

References

1. Tobin, M. J. et al. Breathing patterns. 1. Normal subjects. *Chest*. **84**, 202–205 (1983).
2. Tobin, M. J. et al. Breathing patterns. 2. Diseased subjects. *Chest*. **84**, 286–294 (1983).
3. Tobin, M. J. Why physiology is critical to the practice of medicine: A 40-year personal perspective. *Clin. Chest. Med.* **40**, 243–257 (2019).
4. Tulaimat, A., Gueret, R. M., Wisniewski, M. F. & Samuel, J. Association between rating of respiratory distress and vital signs, severity of illness, intubation, and mortality in acutely ill subjects. *Respir. Care*. **59**, 1338–1344 (2014).
5. Singer, M. et al. The third international consensus definitions for sepsis and septic shock (Sepsis-3). *JAMA*. **315**, 801–810 (2016).
6. Smith, G. B., Prytherch, D. R., Meredith, P., Schmidt, P. E. & Featherstone, P. I. The ability of the National Early Warning Score (NEWS) to discriminate patients at risk of early cardiac arrest, unanticipated intensive care unit admission, and death. *Resuscitation*. **84**, 465–470 (2013).
7. Garrido, D., Assioun, J. J., Keshishyan, A., Sanchez-Gonzalez, M. A. & Goubran, B. Respiratory rate variability as a prognostic factor in hospitalized patients transferred to the intensive care unit. *Cureus* **10**, e2100.
8. Seely, A. J. E. et al. Do heart and respiratory rate variability improve prediction of extubation outcomes in critically ill patients? *Crit. Care*. **18**, R65 (2014).
9. American Thoracic Society/European Respiratory Society. ATS/ERS Statement on respiratory muscle testing. *Am. J. Respir. Crit. Care Med.* **166**, 518–624 (2002).
10. Tulaimat, A., Trick, W. E. & DiapHRaGM A mnemonic to describe the work of breathing in patients with respiratory failure. *PLoS One* **12**, (2017).
11. Tulaimat, A., Patel, A., Wisniewski, M. & Gueret, R. The validity and reliability of the clinical assessment of increased work of breathing in acutely ill patients. *J. Crit. Care*. **34**, 111–115 (2016).
12. Laveneziana, P. et al. ERS statement on respiratory muscle testing at rest and during exercise. *Eur. Respir. J.* **53**, 1801214 (2019).
13. Tobin, M. J. Breathing pattern analysis. *Intensive Care Med.* **18**, 193–201 (1992).
14. Cyphers, V. E. et al. Labored breathing pattern: An unmeasured dimension of respiratory pathophysiology. 01.27.24301872 Preprint at <https://doi.org/10.1101/2024.01.27.24301872> (2024).
15. Ashe, W. B. et al. Analysis of respiratory kinematics: A method to characterize breaths from motion signals. *Physiol. Meas.* **43**, 015007 (2022).
16. Berger, R. D., Akselrod, S., Gordon, D. & Cohen, R. J. An efficient algorithm for spectral analysis of heart rate variability. *IEEE Trans. Biomed. Eng.* **33**, 900–904 (1986).
17. Vincent, J. L. et al. The SOFA (Sepsis-related Organ Failure Assessment) score to describe organ dysfunction/failure. On behalf of the Working Group on Sepsis-Related Problems of the European Society of Intensive Care Medicine. *Intensive Care Med.* **22**, 707–710 (1996).
18. Gadrey, S. M. et al. The relationship between acuity of organ failure and predictive validity of sepsis-3 criteria. *Crit. Care Explorations*. **2**, e0199 (2020).
19. Gadrey, S. M. et al. Imputation of partial pressures of arterial oxygen using oximetry and its impact on sepsis diagnosis. *Physiol. Meas.* **40**, 115008 (2019).
20. Gadrey, S. M. et al. Overt and occult hypoxemia in patients hospitalized with COVID-19. *Crit. Care Explorations*. **5**, e0825 (2023).
21. Forgy, E. Cluster analysis of multivariate data: efficiency versus interpretability of classifications. *Biometrics*. **21** (3), 768–769 (1965). JSTOR 2528559.
22. MacQueen, J. Some methods for classification and analysis of multivariate observations. *Proceedings of 5th Berkeley Symposium on Mathematical Statistics and Probability*. Vol. 1. University of California Press. 5.1, 281–298 (1967).
23. Gibson, W. A. Three multivariate models: Factor analysis, latent structure analysis, and latent profile analysis. *Psychometrika*. **24**, 229–252 (1959).
24. Oberski, D. Mixture models: Latent profile and latent class analysis, in *Modern Statistical Methods for HCI* (eds Robertson, J. & Kaptein, M.) 275–287 (Springer International Publishing, Cham, 2016). https://doi.org/10.1007/978-3-319-26633-6_12.

25. Scrucca, L., Fop, M., Murphy, T. B. & Raftery, A. E. mclust 5: Clustering, classification and density estimation using Gaussian finite mixture models. *R J.* **8**, 289–317 (2016).
26. Aujesky, D. & Fine, M. J. The pneumonia severity index: A decade after the initial derivation and validation. *Clin. Infect. Dis.* **47**, S133–S139 (2008).
27. Papiris, S., Kotanidou, A., Malagari, K. & Roussos, C. Clinical review: Severe asthma. *Crit. Care.* **6**, 30–44 (2002).
28. Philip, K. E. J. et al. The accuracy of respiratory rate assessment by doctors in a London teaching hospital: A cross-sectional study. *J. Clin. Monit. Comput.* **29**, 455–460 (2015).
29. Latten, G. H. P., Spek, M., Muris, J. W. M., Cals, J. W. L. & Stassen, P. M. Accuracy and interobserver-agreement of respiratory rate measurements by healthcare professionals, and its effect on the outcomes of clinical prediction/diagnostic rules. *PLoS One.* **14**, e0223155 (2019).
30. Pneumonia. <https://www.who.int/news-room/fact-sheets/detail/pneumonia>
31. ARIDA (Acute Respiratory Infection Diagnostic Aid.). <https://www.unicef.org/innovation/arida>
32. Khan, A. M. et al. Accuracy of non-physician health workers in respiratory rate measurement to identify paediatric pneumonia in low- and middle-income countries: A systematic review and meta-analysis. *J. Glob Health* **12**, 04037 .
33. Andersen, L. W. et al. Acute respiratory compromise on inpatient wards in the United States: Incidence, outcomes, and factors associated with in-hospital mortality. *Resuscitation.* **105**, 123–129 (2016).
34. Bedoya, A. D. et al. Unanticipated respiratory compromise and unplanned intubations on general medical and surgical floors. *Respir Care.* **65**, 1233–1240 (2020).
35. Steyerberg, E. W., Eijkemans, M. J. & Habbema, J. D. Stepwise selection in small data sets: a simulation study of bias in logistic regression analysis. *J. Clin. Epidemiol.* **52**, 935–942 (1999).
36. Steyerberg, E. W., Schemper, M. & Harrell, F. E. Logistic regression modeling and the number of events per variable: selection bias dominates. *J. Clin. Epidemiol.* **64**, 1464–1465 (2011). author reply 1463–1464.

Acknowledgements

We thank Dr. Mark Sochor, Dr. Thomas Hartka, Ashley Simpson, Anjali Kapil, and Alexander Schwartz of UVA's Emergency Medicine Research Office for their invaluable help with patient enrollment and data collection. We thank Sharon Krueger, program director of the Ivy Foundation's Biomedical Innovation Fund for her advice and support. We thank David Chen, director of UVA's Coulter Translational Research Partnership, for his role in establishing and supporting this multidisciplinary collaboration.

Author contributions

Conceptualization: SMG, WBA, RDW, SJR, JRM; Methodology: SMG, WBA, AJB, RDW, SJR, JRM; Investigation: SMG, WBA, BDM, SMP, JNS, SEI, CJH; Visualization: SMG, WBA; Funding acquisition: SMG, WBA, RDW, SJR, JRM; Supervision: SMG, AJB, RDW, SJR, JRM; Writing – original draft: SMG, WBA; Review/editing: All.

Declarations

Competing interests

SMG, WBA, RDW, SJR, and JRM are co-inventors in United States Patent Application Serial No. 18/018,469 for “METHODS, SYSTEMS, AND COMPUTER READABLE MEDIA FOR ANALYZING RESPIRATORY KINEMATICS”. Other authors declare that they have no competing interests.

Ethical approval

This study was funded by the Ivy foundation COVID-19 translational research fund. It was approved by University of Virginia Health Sciences Institutional Review Board (study number 20844).

Additional information

Supplementary Information The online version contains supplementary material available at <https://doi.org/10.1038/s41598-024-77778-9>.

Correspondence and requests for materials should be addressed to S.M.G.

Reprints and permissions information is available at www.nature.com/reprints.

Publisher's note Springer Nature remains neutral with regard to jurisdictional claims in published maps and institutional affiliations.

Open Access This article is licensed under a Creative Commons Attribution-NonCommercial-NoDerivatives 4.0 International License, which permits any non-commercial use, sharing, distribution and reproduction in any medium or format, as long as you give appropriate credit to the original author(s) and the source, provide a link to the Creative Commons licence, and indicate if you modified the licensed material. You do not have permission under this licence to share adapted material derived from this article or parts of it. The images or other third party material in this article are included in the article's Creative Commons licence, unless indicated otherwise in a credit line to the material. If material is not included in the article's Creative Commons licence and your intended use is not permitted by statutory regulation or exceeds the permitted use, you will need to obtain permission directly from the copyright holder. To view a copy of this licence, visit <http://creativecommons.org/licenses/by-nc-nd/4.0/>.

© The Author(s) 2024